Sains Malaysiana 54(1)(2025): 225-242
http://doi.org/10.17576/jsm-2025-5401-18

Sequestration of Doxycycline and Mefenamic Acid from Liquid Phase Using 1,3-Diaminopropane Modified Poly(Acrylonitrile-Acrylic Acid): Isotherm, Kinetic and Mechanism Studies

(Penyerapan Doksisiklin dan Asid Mefenamik daripada Fasa Cecair Menggunakan 1,3-Diaminopropane Poli(Akrilonitril Asid-Akrilik) Terubah Suai: Kajian Isoterma, Kinetik dan Mekanisme)

FATIMAH LEE[1], SITI NURUL AIN MD JAMIL[1,2,*], NUR NIDA SYAMIMI SUBRI[1], ABEL ADEKANMI ADEYI[3,4] & RUSLI DAIK[5,6]

[1]*Department of Chemistry, Faculty of Science, Universiti Putra Malaysia, 43400 UPM Serdang, Selangor, Malaysia*
[2]*Centre for Foundation Studies in Science of Universiti Putra Malaysia, 43400 UPM Serdang, Selangor, Malaysia*
[3]*Department of Chemical and Environmental Engineering, Faculty of Engineering, Universiti Putra Malaysia, 43400 UPM Serdang, Selangor, Malaysia*
[4]*Department of Chemical and Petroleum Engineering, College of Engineering, Afe Babalola Ado-Ekiti (ABUAD), PMB 5454, Ado-Ekiti 360211, Ekiti State, Nigeria*
[5]*Department of Chemical Sciences, Faculty of Science and Technology, Universiti Kebangsaan Malaysia, 43600 UKM Bangi, Selangor, Malaysia*
[6]*Institute of Microengineering and Nanoelectronics, Universiti Kebangsaan Malaysia, 43600 UKM Bangi, Selangor, Malaysia*

Received: 20 August 2024/Accepted: 30 October 2024

ABSTRACT

Accumulation of pharmaceutical residues in aquatic environment due to daily consumption by humans and animals for diseases treatment results in alarming long-term effects. This study evaluates the adsorption potential of a polymer-based adsorbent, 1,3-diaminopropane-modified poly(acrylonitrile-acrylic acid) (DAP-poly(ACN/AA)), for the uptake of doxycycline (DOX) and mefenamic acid (MEFA) from aqueous solution. The chemical modification of poly(ACN/AA) copolymer with DAP was successful as suggested by the FTIR spectra and microanalysis results. The SEM analysis showed that the modified copolymer has larger particle size, which was 156 nm as compared to that of poly(ACN/AA) copolymer (133 nm). The influence of adsorbent dosage, contact time, pH and initial concentration on the adsorption of DOX and MEFA compounds were investigated. The kinetic studies of DOX and MEFA was fitted well to pseudo-second-order model with chemisorption being the rate-controlling step. The equilibrium isotherm has its fitness in the following order: Langmuir model > Freundlich model > Temkin model. The maximum adsorption capacities for DOX and MEFA were 210.4 mg/g and 313.7 mg/g, respectively. The excellent high sorption capacity suggest that DAP-modified poly(ACN/AA) copolymer is a potential adsorbent for the treatment of DOX and MEFA bearing effluent in adsorption system.

Keywords: Copolymer; doxycycline; isotherm; kinetic pharmaceutical; mefenamic acid; poly(acrylonitrile-*co*-acrylic acid)

ABSTRAK

Pengumpulan sisa farmaseutikal dalam persekitaran akuatik akibat penggunaan harian oleh manusia dan haiwan untuk rawatan penyakit mengakibatkan kesan jangka panjang yang membimbangkan. Kajian ini menilai potensi penjerapan bahan penjerap berasaskan polimer, 1,3-diaminopropan-terubahsuai poli(akrilonitril-asid akrilik) (DAP-poli(ACN/AA)) untuk mengeluarkan doksisiklin (DOX) dan asid mefenamik (MEFA) daripada larutan akueus. Pengubahsuaian kimia kopolimer poli(ACN/AA) dengan DAP berjaya seperti mana dicadangkan daripada spektra FT-IR dan keputusan analisis-mikro. Analisis SEM menunjukkan bahawa kopolimer yang diubah suai mempunyai saiz zarah yang lebih besar, iaitu 156 nm berbanding dengan kopolimer poli(ACN/AA) (133 nm). Pengaruh dos penjerap, masa sentuhan, pH dan kepekatan awal ke atas penjerapan sebatian DOX dan MEFA telah dikaji. Kajian kinetik DOX dan MEFA telah dipadankan dengan baik pada model pseudo-tertib-kedua dengan penjerapan kimia sebagai langkah mengawal kadar. Isoterma keseimbangan mempunyai kesesuaiannya dalam susunan berikut: Model Langmuir > Model Freundlich > Model Temkin. Kapasiti penjerapan maksimum untuk DOX dan MEFA masing-masing ialah 210.4 mg/g dan 313.7 mg/g. Kapasiti penjerapan tinggi yang sangat baik menunjukkan bahawa kopolimer poli(ACN/AA) diubah suai DAP ialah penjerap yang berpotensi untuk rawatan efluen yang mengandungi DOX dan MEFA dalam sistem penjerapan.

Kata kunci: Asid mefenamik; doksisiklina; isoterma; kinetik farmaseutikal; kopolimer; poli(akrilonitril-*ko*-asid akrilik)

INTRODUCTION

The urban water cycle of over 70 countries in the world, is severely infested by pharmaceuticals of broad spectrum of drug classes, particularly non-steroidal anti-inflammatory drugs (NSAIDs) and antibiotics due to the increasing human consumption to treat various diseases, aquaculture activities, medicine production facilities and limitation in wastewater treatment process (Mohd Hanafiah et al. 2023; Perumal et al. 2024). The consumed drugs were excreted in the form of 50 - 90% active metabolites from total consumption into wastewater treatment plants (WWTPs) (Dolatabadi, Ahmadzadeh & Ghaneian 2020). The current wastewater treatment technologies in Malaysia were not designated to thoroughly remove pharmaceutical residues (PRs) due to its chemical stability towards degradation, complex chemical structure, and formation of metabolites (Hanafiah et al. 2024). Thus, the residues were discharged at the end point along with effluent and influent into the waterways and used as water source for human use. Although PRs is detected at trace level, the exposure to the residue on daily basis *via* contaminated drinking water, aquaculture products and water, can lead to serious health threats, changes in hormones of aquatic organisms, antibiotic resistance and even fatality over the time (Samal, Mahapatra & Hibzur Ali 2022). Therefore, selective method and material must be developed to solve this detrimental issue.

Mefenamic acid (MEFA) is a common and most effective over the counter NSAIDs used in Asia-Pacific region as a pain reliever for menstrual cramps, which has been frequently detected in water environment due to low biodegradability, resulting in low removal efficiency in WWTPs (Al-Ameer, Hashim & Taha 2022; Lai et al. 2018). MEFA was detected at concentrations of 595.2 ng/L in effluent samples of Sungai Langat, Selangor (Al-Odaini et al. 2013). Owing to the fact that MEFA presents as unchanged metabolites in water bodies, prolonged exposure to contaminated drinking water may lead to serious gastrointestinal events, such as bleeding and ulcer. On the other hand, doxycycline (DOX), a tetracycline antibiotic is frequently prescribed to treat acne vulgaris, urinary and respiratory tract infections and sexually transmitted infections, and is intensively used in aquaculture farms to treat wide range of bacterial infections in the form of mixed-medicated feed, where healthy fishes were also fed with the same feed (Thiang et al. 2021; Malaysian Health Technology Assessment Section 2022). As a result of high usage, DOX residues may absorb into gastrointestinal tract of aquaculture products, accumulate in their tissues and lead to the spread of antibiotic-resistant genes (ARGs) among bacteria through gene transfer producing antibiotic resistant bacteria (ARBs) (Hua et al. 2022). ARBs can be transmitted from animals to human via food-borne route, where prolonged consumption of ARBs contaminated food may reduce the effectiveness of antimicrobial medicines. With that, infections become difficult or impossible to treat leading to an increase of disease spread risk, severe illness and deaths (World Health Organization, 2023). In 2020, DOX was detected at concentrations up to 234 ng/L in aquaculture farms across Peninsular Malaysia (Thiang et al. 2021). Thus, there is an urgent need to effectively remove MEFA and DOX residues from aqueous environment to address this alarming threat to public health.

In order to remove MEFA and DOX from water environment, several methods have been developed such as electrocoagulation, adsorption, ion exchange, biological oxidation, reverse osmosis and photocatalytic degradation. Among these methods, adsorption method has been proven to be an effective way to remove pharmaceutical residues from wastewater owing to its high removal capacity, inexpensive, easy handling, and variation of adsorbents. The commonly used adsorbents in previous studies were biomass based activated carbon (AC), magnetic nanomaterial such as Fe_3O_4 nanoparticles and silica-based sorbents. Although AC is regarded as an excellent adsorbent due to its large surface area, high adsorption capacity (up to 99% removal) and microporous structure (Mudhoo et al. 2019), AC lack of selectivity towards specific pollutants, which means AC is able to capture most contaminants including natural organic matter (NOM) in wastewater resulting in fouling, leading to low removal of the targeted pharmaceutical residues (Hassan & Hawkyard 2007; Husien et al. 2022). Despite the fact that magnetic Fe_3O_4 nanoparticles adsorbents were proven to have high adsorption capacity for water pollutants (Habila et al. 2023), its utilisation was limited at laboratory scale due to high cost and complicated modification method for large-scale industrial applications (Gao 2019). On the contrary, polymeric adsorbents overcome the disadvantages of the conventional adsorbents mentioned due to their great selectivity, ease of chemical modification, easy regeneration of adsorbent, stable across entire pH range, cost-effective, economical feasible and high removal efficiency (Panic et al. 2013; Subri et al. 2018). Polymeric adsorbents such as polyacrylonitrile (PACN) has been utilised for various application due to the presence of pendant nitrile group (Zahri et al. 2015). However, PACN is inefficient adsorbent due to the presence of polar cyano groups (-C≡N) that leads to intermolecular attractions between the nitrile groups resulting in high nitrile-nitrile dipolar interaction along the polymer chain (Sruthi & Anas 2020). For that reason, PACN has low absorption, high hydrophibicity and lack of surface functionality for effective adsorption process. Therefore, PACN is copolymerised with vinyl and acrylic monomers such as acrylic acid (AA) that contains carboxyl groups (-COOH) that has contrast nature from cyano groups (Zahri et al. 2015). Carboxyl group can participate in hydrogen bonding, ionic interaction and electrostatic attractions. The resulting copolymer, poly(ACN/AA) with the presence of -COOH disrupts the strong intermolecular attractions of cyano groups (Jamil, Daik & Ahmad 2014), consequently improving its surface functionality to interact

with polar compounds for better adsorption process. This may also improve adsorbent's hydrophilicity as well as producing pervaporation and antifouling properties for wastewater treatment (Adeyi et al. 2019).

In this study, acrylonitrile (ACN) was copolymerised with acrylic acid (AA) by using redox polymerisation method to produce poly(ACN/AA) copolymer. ACN-based polymers can be chemically modified with various modification reagents, such as hydroxyl amine (amidoxime functional group), hydrazine derivatives, amines and aminoalcohols due to the presence of highly reactive -C≡N groups to further enhance its physicochemical features, as well as improving adsorption efficiency (Eniola et al. 2022). Sruthi and Anas (2020) stated that amine containing resins demonstrates excellent adsorption properties through its chelation mechanism. Rahimi et al. (2019) conducted a study on amine-modification of carboxylated carbon nanotubes using 1,3-diaminopropnane (DAP) where the adsorption capacity of CO_2 was enhanced from 48.49 mg/g to 92.71 mg/g after amine modification. However, there was limited studies on the utilisation of amine-modified ACN-based polymer as an adsorbent for the adsorption of pharmaceutical residues. Thus, this study focuses on the chemical modification of -C≡N groups in poly(ACN/AA) copolymer into diamine polar groups (-NH_2 and =N-H) using DAP, and its application as adsorbent towards MEFA and DOX removal from liquid phase. The modified polymer sorption capacity and mechanism was investigated through kinetic, and isotherm analyses.

METHODOLOGY

MATERIALS

The reagents used for the polymer synthesis were acrylonitrile (ACN 99%; stabilised with hydroquinone monomethyl ether for synthesis, MERCK, Darmstadt, Germany) and acrylic acid (AA; 98% grade, extra pure, ACROS ORGANICS). The purification of ACN and AA were performed by passing the monomers, respectively, through a short column of aluminium oxide (90 active neutral, MERCK, Darmstadt, Germany) with glass wool to remove impurities. The initiators used in the polymerization were sodium bisulphate (R&M Chemicals, UK) and potassium persulphate (SYSTERM). 1,3-diaminopropane (99% grade, Acros Organics) was used as modification reagent. Methanol (R&M Chemicals, UK) and ethanol (R&M Chemicals, UK) were used to precipitate and wash polymers produced during filtration. Sodium chloride (HmbG Chemicals) was used as solvent in point zero charge determination of adsorbents. Mefenamic acid (MEFA) and doxycycline hydrochloride (DOX) were used as adsorbates for the adsorption study.

INSTRUMENTATION

Fourier transform infrared spectrophotometer INVENIO R (Bruker, Germany) and CHNS-932 LECO (TruSpec CHN, USA) were employed to analyse the chemical structure of polymers. The morphological structure of copolymer and modified polymer were analysed with a Scanning Electron Microscope (JEOL JSM 6360 LA, Japan). Thermogravimetric analysis (TGA) was executed using Perkin Elmer (STA6000, U.S.A.), from 50 °C to 800 °C at 10 °C/min under nitrogen atmosphere. Brunauer-Emmett-Teller (BET) analysis was conducted by using Micrometrics Instrument Corporation, ASAP 2010 (USA) surface analyser. The point zero charge was determined by using pH meter (Santorius PB-19), where initial pH and final pH were recorded to plot graph of ΔpH (pH_{final} - $pH_{initial}$) against initial pH (Abu Rumman et al. 2021).

SYNTHESIS OF PACN AND POLY(ACN/AA)

Redox polymerization was carried out in a three-neck round bottom flask, connected to a water condenser and nitrogen gas, where silicone oil was used as heating bath. The monomers, acrylonitrile and acrylic acid were purified beforehand, by passing them through a short column of neutral aluminium oxide (Al_2O_3) with glass wool. The reaction medium, 200 mL of deionized water was purged with nitrogen gas at 40 °C for 30 min. Then, ACN and AA were added into the reaction medium, followed by 2.09 g (0.02 mol) of sodium bisulphate (SBS) and 2.16 g (0.008 mol) of potassium persulphate (KPS), as initiators. The reaction temperature was increased to 60 °C and was stirred at 200 rpm using a magnetic stirrer. The amount of ACN and AA monomers added were according to the comonomer compositions (ACN:AA %mol) of 100:0, 97:3, 95:5, 93:7 and 90:10. The procedures were repeated for all comonomer compositions. In the copolymer system, ACN content is maintained at no less than 90%. Increasing AA content to 15-20% leads to the formation of a light, brittle copolymer. After 3 h of polymerisation reaction, the white cloudy solution formed was precipitated in excess methanol for an hour before being filtered, rinsed and washed with methanol and deionized water. The polymer was then oven-dried in vacuum at 45 °C until constant weight was obtained. This polymerization method was as reported by Zahri et al. (2015).

CHEMICAL MODIFICATION POLY(ACN/AA) WITH 1,3-DIAMINOPROPANE (DAP)

The surface functionalization of the synthesized 97:3 mol% poly(ACN/AA) was carried out under a reflux setup using a round-bottom flask. 9.0 mL of 1,3-diaminopropane (DAP) and ethanol-water mixture (1:2 vol.%) were added into the

flask and stirred continuously at 200 rpm for 30 min at 80 °C. Then, 3.0 g of poly(ACN/AA) was added into the flask and the mixtures were allowed to react for 5 h at 80 °C. The yellowish cloudy solution, DAP-modified poly(ACN/AA) was filtered, rinsed with ethanol-deionized water (1:2 vol%) solution and oven-dried to a constant weight at 50 °C. This modification method was referred from Adeyi et al. (2019). The chemical modification route of poly(ACN/AA) is illustrated in Scheme 1.

ADSORPTION OF DOX AND MEFA USING DAP-MODIFIED POLY(ACN/AA)

1 g of each pharmaceutical compound was dissolved in 1000 mL of double-distilled water to create the stock solution (1000 mg/L) of DOX and MEFA. Forty mg of DAP-modified poly(ACN/AA) was added into 20 mL of 30 ppm of DOX solution in conical flask. The solution was shaken at 100 rpm, for 120 min at room temperature (25 °C). Then, the solution was centrifuged for 5 min at 4000 rpm. 3 mL aliquot of the supernatant was withdrawn and filtered using 0.2 µm Millipore filter syringe. The same procedures were repeated to study the adsorption of MEFA by DAP-modified poly(ACN/AA). The filtered solution was then analysed using Ultraviolet-visible double beam spectrophotometer Dynamica HALODB-20 at the maximum wavelength of 370 nm and 344 nm, for DOX and MEFA solution, respectively, at predetermined intervals during the experiment. The percentage removal, R of DOX and MEFA can be expressed as Equation (1):

$$R = \frac{C_o - C_e}{C_o} \times 100\% \quad (1)$$

where C_o is the initial concentration of the solution; and C_e is the equilibrium adsorbate concentration in solution (ppm).

ADSORPTION ISOTHERMS

40 mg of DAP-modified poly(ACN/AA) was added to varying initial concentrations of DOX (10 ppm to 100 ppm) and MEFA (5 ppm to 80 ppm) solutions, respectively, to determine the adsorption isotherms. The adsorption capacity at equilibrium, q_e was determined using Equation (2):

$$q_e = \frac{C_o - C_e}{m} \times V \quad (2)$$

where q_e (mg/g) is the amount of adsorbate being adsorbed on per gram of adsorbent at equilibrium; C_o and C_e are the initial and equilibrium concentration of adsorbate in solution (ppm), respectively; m (g) is the amount of adsorbent used; and V (L) is the volume of the solution.

In this study, Langmuir, Freundlich and Temkin isotherm model are used to investigate the equilibrium relationship between the quantity of drugs adsorbed on adsorbent surface and to determine the mechanism of adsorption reactions. The linearised form of Langmuir, Freundlich and Temkin isotherm models and separation factor, R_L can be expressed as Equations (3), (4), (5) and (6), respectively (Adeyi et al. 2019):

$$\frac{1}{q_e} = \frac{1}{C_e}\frac{1}{K_L \cdot q_m} + \frac{1}{q_m} \quad (3)$$

$$\log q_e = \frac{1}{n} \log C_e + \log K_F \quad (4)$$

$$q_e = B_T \ln K_T + B_T \ln C_e \quad (5)$$

$$RL = \frac{1}{1 + K_L \cdot C_o} \quad (6)$$

where q_e is the amount of drugs per unit mass of adsorbent at equilibrium (mg/g); C_e is the equilibrium concentration of drugs (mg/L); K_L is Langmuir constant (L/mg); and q_m is the maximum amount of drugs adsorbed per unit mass of

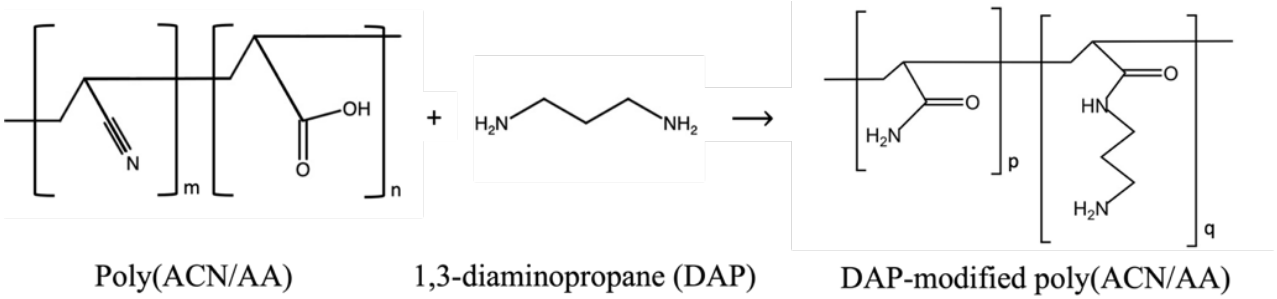

Poly(ACN/AA) 1,3-diaminopropane (DAP) DAP-modified poly(ACN/AA)

SCHEME 1. Chemical modification of poly(ACN/AA) with 1,3-diaminopropane (DAP)

adsorbent for the formation of complete monolayer on the surface of adsorbent (mg/g); n is the heterogeneity factor; K_F is Freundlich constant ((mg/g)/(mg/L)^n); $B_T = \frac{RT}{b}$ is the heat of adsorption associated with Temkin's constant and K_T is the equilibrium binding constant corresponding to the maximum binding energy for the Temkin isotherm (L/mg). R represents the universal gas constant (8.314 J/mol·K), and b is a Temkin isotherm constant (J/mol), while T refers to the absolute temperature of the solution (K).

ADSORPTION KINETICS

Adsorption kinetics of DAP-modified poly(ACN/AA) was studied by varying the contact time (1, 3, 5, 10, 15, 20, 25, 30, 35, 40, 45, 60, 90, and 120 min) with 40 mg of DAP-modified poly(ACN/AA) in DOX and MEFA solutions, respectively. The amount of adorbate being adsorbed by the adsorbent at time *t* was calculated using Equation (7):

$$q_t = \frac{C_o - C_t}{m} \times V \quad (7)$$

where q_t is the amount of adsorbate adsorbed on per gram of adsorbent at time *t*; C_o and C_e are the initial and equilibrium concentration of adsorbate in solution (ppm), respectively; m (g) is the amount of adsorbent used; and V (L) is the volume of the solution.

Pseudo-first order (PFO) and pseudo-second order (PSO) models are used to investigate the adsorption kinetics of DOX and MEFA onto DAP-modified poly(ACN/AA). PFO and PSO kinetic model equation in linearised form is expressed as Equations (8) and (9), respectively (Wang & Guo 2020).

$$\log(q_e - q_t) = \log q_e - \frac{k_1}{2.303} t \quad (8)$$

$$\frac{t}{q_t} = \frac{1}{k_2 \cdot q_e^2} + \left(\frac{1}{q_e}\right) t \quad (9)$$

where q_e and q_t are the amounts of drugs adsorbed per unit mass of adsorbent (mg/g) at equilibrium and any time, respectively; k_1 is the pseudo-first order rate constant (1/min); and k_2 is the pseudo-second order rate constant (g/mg min).

RESULTS AND DISCUSSION

PACN AND POLY(ACN/AA) POLYMERIZATION YIELD

The polymerization of PACN and poly(ACN/AA) copolymer produced a white cloudy solutions after 1 hour of reaction time. PACN (homopolymer) has the highest percentage yield as a result of containing only acrylonitrile (ACN) monomers and no incorporation of any comonomer that may interrupt the polymerisation reaction (Zahri et al. 2015). Meanwhile, poly(ACN/AA) 97:3 has the lowest percentage yield among the copolymer. This might be due to the low amount of acrylic acid (AA) containing carboxyl group (-COOH) used, that is insufficient to form a long polymer chain (Zahri et al. 2015). As the amount of AA ratio increased, the yields were also increased, with 74.16% yield for 95:5 feed ratio and 91.83% yield for 93:7 feed ratio. This might be associated to the higher amount of AA used, thus adequate amount of -COOH functional groups were introduced to form longer polymer chain. However, the percentage yield of 90:10 feed ratio decreases to 80.66%, which due to the excess of -COOH groups present on polymerization system, hindering the formation of polymer chain and slows down the polymerization reaction rate according to Zahri et al. (2015). Based on the highest percentage yield, feed ratio 93:7 was selected for chemical modification with DAP.

AMINE DENSITY OF DAP-MODIFIED POLY(ACN/AA) COPOLYMER

Amine density of DAP-modified poly(ACN/AA) copolymer can be calculated using Equation (10), according to Saber et al. (2021). This is to determine the amount of DAP amine group incorporated on the surface of the modified copolymer.

$$\text{Amine density (mmol/g)} = \frac{W_{MP} - W_P}{W_{MP}} \times \frac{1000}{MW} \quad (10)$$

where W_{MP} is the dry weight of DAP-modified poly(ACN/AA) copolymer (g); W_P is the poly(ACN/AA) copolymer (g) used to be modified; and MW is the molecular weight of DAP (74.13 g/mol).

After 3.0 g of poly(ACN/AA) copolymer was modified with DAP, 4.6525 g of DAP-modified poly(ACN/AA) copolymer was obtained. Therefore, by using Equation (10), the yield of amine density of DAP-modified poly(ACN/AA) copolymer was 4.9710 mmol/g while for poly(ACN/AA) was 0.0 mmol/g due to the absence of amine functionalities in poly(ACN/AA). The weight of modified adsorbent increased as expected, due to new functional groups present in the polymer chain. The amino groups (-NH_2) in DAP are deprotonated to form a positively charged species. Similarly, Saber et al. (2021) reported in their work that the amine density of trimethylamine (TMA) functionalized fiber was 2.8430 mmol/g which was higher as compared to that non-functionalized fiber. This shows that DAP-modified copolymer has higher amine density, which is expected to have a better adsorption efficiency towards adsorbates.

CHARACTERIZATION OF PACN, POLY(ACN/AA) AND DAP-MODIFIED POLY(ACN/AA)

Figure 1 shows the FTIR spectra of PACN, poly(ACN/AA) and DAP-modified poly(ACN/AA). The FTIR spectrum of PACN showed a strong absorption band at 2242 cm^{-1}, corresponds to the stretching vibration of nitrile group (-C ≡ N) (Nandiyanto, Ragadhita & Fiandini 2023). This confirms the presence of cyano functional group in the polymer backbone. The absorption band at 2937 cm^{-1} indicates the presence of aliphatic -CH stretching. The FTIR spectrum of poly(ACN/AA) copolymer showed a new absorption band at 1730 cm^{-1} represents carbonyl group stretching vibration (-C=O) of acrylic acid component (Mohamad et al. 2023), which confirms a successful copolymerization of AA and AN monomers. After chemical modification with DAP, the FTIR spectrum of DAP-modified poly(ACN/AA) exhibits several notable changes compared to the unmodified copolymer. The disappearance of the -C≡N stretching band at 2243 cm^{-1} (from nitrile group) indicates the successful chemical modification of the nitrile group *via* base-catalysed hydrolysis where -C≡N group reacts with hydroxide ion ($^{-}$OH) to yield hydroxyimine and amide group (tautomerisation). Therefore, an absorption band appears at 1654 cm^{-1}, confirms the presence of an open-chain imino (-C=N-) group from hydroxyimine which is a result of the reaction between the nitrile group and $^{-}$OH. Interestingly, the 1654 cm^{-1} absorption peak may also overlap with the amide stretching band (-C(O)-N-C-) (Nandiyanto, Ragadhita & Fiandini 2023) that arises from the chemical modification of the carboxylic group from the acrylic acid component with DAP, leading to the formation of an amide group. This observation is supported by mechanism illustrated by McMurry (2023) on the chemistry and reaction of nitriles that involves nucleophilic addition of hydroxide ion to the polar -C≡N bond. Furthermore, the absorption band at 3327 cm^{-1} is attributed to the amine group (-NH_2), which may overlap with the -OH stretching of hydroxyimine tautomers in DAP-modified poly(ACN/AA). This assertion of -OH and -NH_2 overlapping is in agreement with previous reports (Nandiyanto, Ragadhita & Fiandini 2023; Santos et al. 2014; Slavov et al. 2024). The appearance of the 1317 cm^{-1} absorption band is associated with the stretching vibrations of the C-N bond from amine functionality that further confirming the successful incorporation of DAP into the poly(ACN/AA) chain. These spectroscopic observations collectively indicate the successful modification of the poly(ACN/AA) with DAP, forming the desired DAP-modified poly(ACN/AA). Note that, a shift of C=O stretching of AA in copolymer spectrum; from 1730 cm^{-1} to 1654 cm^{-1} was attributed to the overlapping of C=O of amide stretching band and -C=N (imino group) of hydroxyimine as a result of the reaction of -COOH and DAP.

The proposed mechanism for the chemical modification of poly(ACN/AA) with DAP, based on the FTIR spectra, is shown in Figure 2, in which nucleophilic addition may have occurred, with DAP acting as a nucleophile that attacks the carbonyl group to form an alkoxide ion (a reactive intermediate). Since the hydroxide ion ($^{-}$OH) is a good leaving group, the intermediate subsequently loses the OH group, resulting in an amide functionality with -OH as a by-product. Meanwhile, the conversion of the nitrile group into an amide group occurs through base-catalyzed hydrolysis, which involves the nucleophilic addition of a hydroxide ion to the polar -C≡N bond (McMurry 2023). This reaction produces an imine anion, which is then protonated by water to yield a hydroxyimine group. Following this, tautomerization of the hydroxyimine produces the amide group. The $^{-}$OH ions acting as nucleophiles may originate from the ethanol-water mixture used as the solvent and from the by-products of the modification of poly(ACN/AA) with DAP.

Figure 3(a)-3(c) shows SEM images of PACN, poly(ACN/AA), and DAP-modified poly(ACN/AA), respectively. In Figure 3(a), the SEM image of PACN appeared to be clusters of agglomerated small particles with a coarse surface, while the particles of poly(ACN/AA) in Figure 3(b) appeared to be more spherical and less agglomerated. The agglomeration was due to intraparticle bonds between ACN and AA monomers, low viscosity of the solution and the complex nature of polymerization reaction (Adeyi et al. 2019). After chemical modification, DAP-modified poly(ACN/AA) particles in Figure 3(c) appeared in the form of a more clear spherical beads with rough surface and even lesser agglomerated, providing a suitable binding sites for the adsorption of adsorbates. Table 1 tabulates the average particle size of PACN, poly(ACN/AA), and DAP-modified poly(ACN/AA) calculated using ImageJ software by measuring the diameter of 50 particles of each polymer. The average particle diameter increases from 133 nm (poly(ACN/AA)) to 156 nm after modification with DAP. This increment and morphologies observation indicates a successful surface modification of DAP by the incorporation of amine group onto the surface of poly(ACN/AA). A similar observation of increase in average particle size was reported by Adeyi et al. (2019) and Rapeia et al. (2014). As shown in Table 1, the nitrogen sorption analysis data obtained for poly(ACN/AA) copolymer and DAP-modified poly(ACN/AA) copolymer. The specific surface area, pore volume and mean pore size of the DAP-modified poly(ACN/AA) (74.10 m^2/g) were notably higher compared with poly(ACN/AA). The modification with DAP appears to have a substantial impact on the structure of the polymer, leading to increased surface area, pore volume, and pore size. This could be due to the incorporation of DAP molecules into the polymer chain, which may disrupt the crystalline structure and create more open spaces for adsorption. Similar observation was reported by Adeyi et al. (2019), where specific surface area and mean pore size of acrylonitrile-acrylic acid copolymer increased from 22.99 m^2/g to 26.31 m^2/g and from 41.60 nm to 47.23 nm, respectively after chemically modified with thiourea (TU).

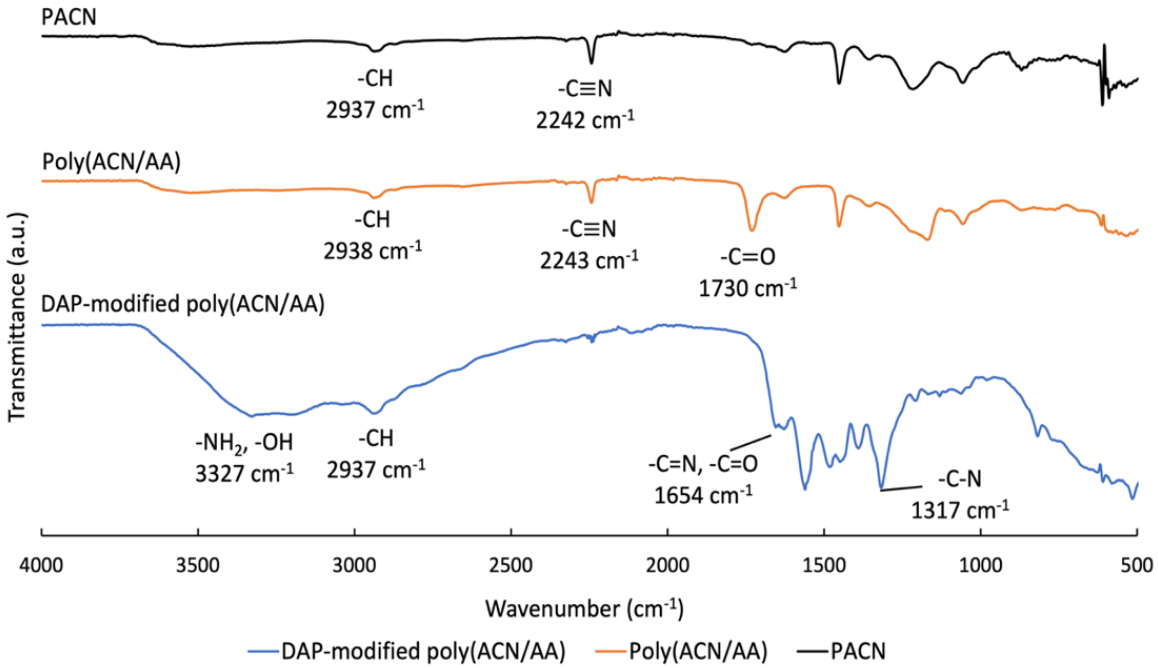

FIGURE 1. FTIR spectra of PACN, poly(ACN/AA) and DAP-modified poly(ACN/AA)

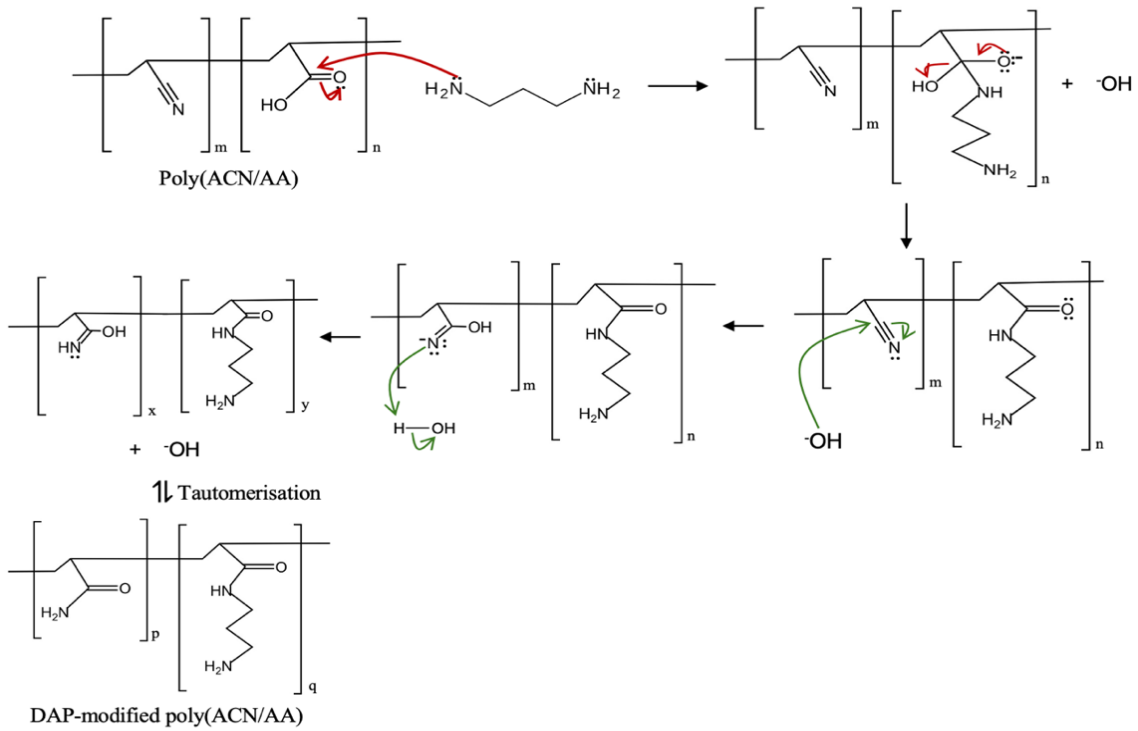

Red colour arrow: Modification carbonyl group; Green colour arrow: Modification of nitrile group

FIGURE 2. Proposed mechanism of chemical modification of poly(ACN/AA) with DAP

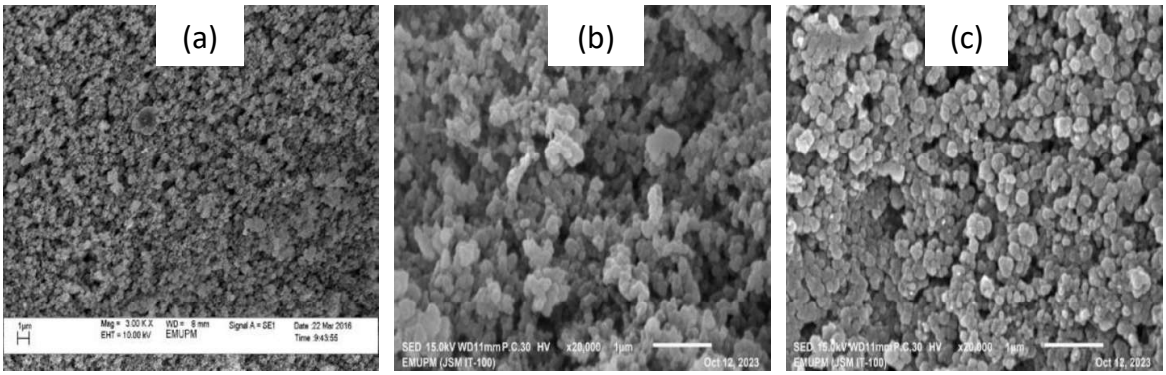

FIGURE 3. SEM images of (a) PACN, (b) Poly(ACN/AA) and (c) DAP-modified poly(ACN/AA)

TABLE 1. Average particle size and BET analysis data of PACN, poly(ACN/AA) and DAP-modified poly(ACN/AA)

Sample	Average particle diameter (nm)	Specific surface area (m^2/g)	Specific pore volume (cm^3/g)	Mean pore size (nm)
Poly(ACN/AA)	133	49.92	0.3862	20.88
DAP-modified poly(ACN/AA)	156	74.10	0.8513	159.24

Elemental microanalysis of the three polymer samples were presented in Table 2. The PACN has a high carbon content (51.79%), which is expected since PACN is a polymer composed mainly of carbon and hydrogen. The copolymer poly(ACN/AA) has a slightly lower carbon content (51.49%) compared to PACN, which might be due to the incorporation of oxygen atoms from acrylic acid. Poly(ACN/AA) modified with DAP shows a significant decrease in carbon content (48.43%), increase in hydrogen content (7.00%) and increase in nitrogen content (20.19%). Increment of nitrogen content in modified copolymer might be contributed by the DAP that consists of amino groups. This suggests that DAP has been incorporated into the polymer backbone, leading to a change in its elemental composition. The low sulfur (S) content in PACN, poly(ACN/AA), and DAP-modified poly(ACN/AA) may result from trace amounts of sulfur introduced by the initiators (SBS and KPS) used in the polymer synthesis process.

Figure 4(a) and 4(b) depicts respectively, the TGA and DTG curve while Table 3 shows the char yield and weight loss of the polymer samples at 800 °C. PACN has the highest char yield at 800 °C (50.82%) followed by poly(ACN/AA) (38.64%) and DAP-modified poly(ACN/AA) (30.13%). This indicates that DAP-modified poly(ACN/AA) has the lowest thermal stability compared to PACN and copolymer. PACN is expected to have the highest thermal stability as the heating of PACN encouraged the cyclization of nitrile groups and formed a ladder structure that helps to retain the polymeric backbone structure from degrading as much as poly(ACN/AA) and DAP-modified poly(ACN/AA). Meanwhile, poly(ACN/AA) copolymer backbone consists of carboxylic acid groups that require less energy for cyclization process whereby the process can be initiated at lower temperature in comparison to PACN, hence it can be observed in Figure 4(a) that poly(ACN/AA) has steeper curve at around 350 °C and consequently having lower thermal stability than PACN (Ismar & Sarac 2016). Additionally, the conversion of nitrile group (-C≡N) in poly(ACN/AA) chain into amide group and conversion of carboxyl group (-COOH) into imine and amide groups with amine group at the terminal end may have caused changes in chemical structure of DAP-modified copolymer resulting in a reduction of thermal stability. The char yield results shows that the modified copolymer has the highest weight loss compared to PACN and poly(ACN/AA). This is expected due to the presence of amide functional group that has interrupted the nitrile arrangement along the PACN backbone and tend to be disrupted during thermal degradation.

The point of zero charge (pH_{PZC}) is a crucial parameter in understanding the characteristics of an adsorbent, as it defines the pH at which the net charge on the surface of the adsorbent is zero. As illustrated in Figure 5, the pH_{PZC} of poly(ACN/AA) is 6.88, whereas for DAP-modified poly(ACN/AA), it is 7.88. Below the pH_{PZC}, the adsorbent surface is positively charged (cationic), while above it, the surface is negatively charged (anionic) (Yadav et al. 2023). In acidic conditions, where there is an excess of protons (H^+), these ions occupy active sites on the adsorbent,

TABLE 2. Elemental microanalysis data of PACN, poly(ACN/AA) and DAP-modified poly(ACN/AA)

Sample	Elemental microanalysis (%)			
	Carbon	Hydrogen	Nitrogen	Sulfur
PACN	51.79	4.80	19.84	2.89
Poly(ACN/AA)	51.49	4.56	19.00	2.47
DAP-modified poly(ACN/AA)	48.43	7.00	20.19	0.04

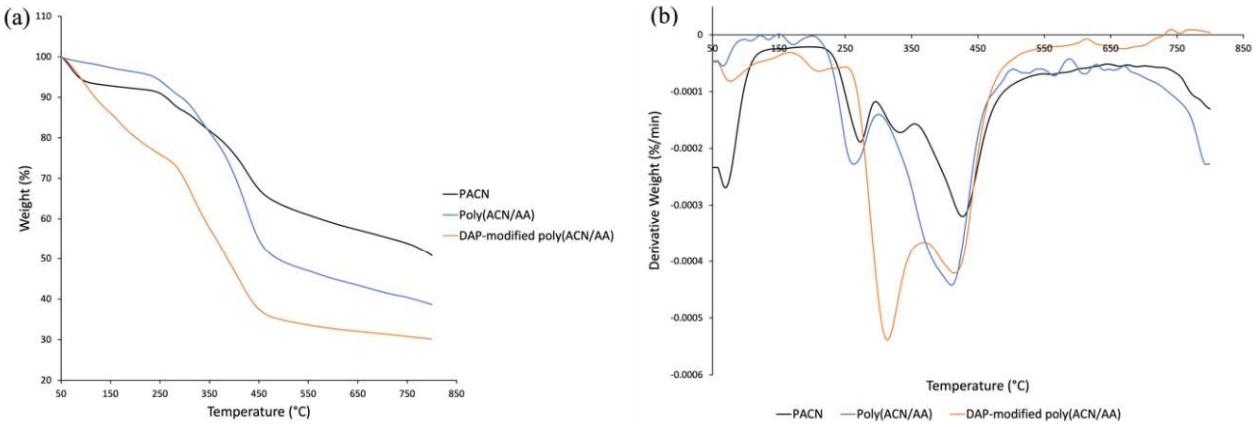

FIGURE 4. (a) TG curve and (b) DTG curve of PACN, poly(ACN/AA) and DAP-modified poly(ACN/AA)

TABLE 3. Char yield and total weight loss of PACN, poly(ACN/AA) and DAP-modified poly(ACN/AA) at 800 °C

Sample	Weight loss (%)	Char yield (%)
PACN	49.18	50.82
Poly(ACN/AA)	61.36	38.64
DAP-modified poly(ACN/AA)	69.87	30.13

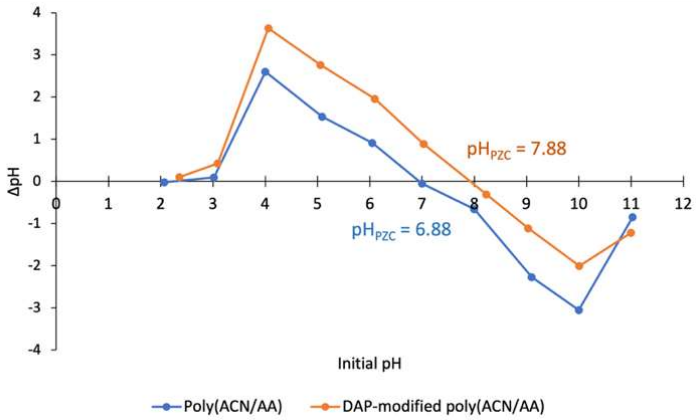

FIGURE 5. pHPZC of poly(ACN/AA) and DAP-modified poly(ACN/AA)

resulting in a positively charged surface. Conversely, in basic conditions, where there is an abundance of hydroxide ions (OH^-), they occupy the active sites, rendering the adsorbent surface negatively charged.

EFFECT OF INITIAL pH

The influence of pH plays an important role towards the adsorption efficiency of DOX and MEFA onto the surface of DAP-modified poly(ACN/AA). Figure 6(a) and 6(b) shows the effect of pH on the percentage removal and quantity of DOX and MEFA adsorbed by DAP-modified poly(ACN/AA), respectively. As shown in Figure 6(a), with the increase of pH from 2 to 10, the percentage removal and sorption capacity also increased, from 17.36% (14.29 mg/g) to 83.02% (68.32 mg/g). Thus, the optimum pH for the adsorption of DOX onto DAP-modified poly(ACN/AA) was pH 10. The pK_a values of adsorbate are considered to explain these results. DOX has three pK_a values (3.5, 7.7 and 9.5) which complicates and affect the adsorption efficiency. At pH $\leq$ 3.5, DOX is protonated and exist in cationic form (DOX^+). Meanwhile, at 3.5 $\leq$ pH $\leq$ 9.5, DOX exists as zwitterions and at pH $\geq$ 9.5, DOX exists in anionic form, which means some of the functional groups are negatively charged (Olusegun & Mohallem 2019). Since the pH_{PZC} of DAP-modified poly(ACN/AA) is 7.88, this means at pH 10, both adsorbent and DOX molecules are negatively charged. The interaction between DAP-modified poly(ACN/AA) and DOX molecules were mainly by hydrogen bonding that contributes to high adsorption of DOX. It is known that doxycycline contains five hydroxyl groups and has three pK_a values (3.5, 7.7, and 9.5). Deprotonation at a high pH (pH > 9.5) occurs only for two OH groups of doxycycline, converting them into alkoxide ions (Yadav, Shah & Malhotra 2024). Thus, doxycycline still has an abundance of OH groups that remain protonated. Therefore, hydrogen bonding is still considered favorable and contributes to its adsorption. Furthermore, high adsorption at pH 10 was obtained also due to the released of -OH group from negative molecules for proton exchange with water (solvent) and formed neutral DOX molecules (equation 11). Then, followed by the interaction of DOX^0 with the functional group on the surface of adsorbent. The interaction was supported by a strong negative charge assists hydrogen bonding (CAHB) resulting in a favourable interaction for adsorption process (Ahmed et al. 2017).

$$DOX^- + H_2O \rightarrow DOX^0 + OH^- \quad (11)$$

As shown in Figure 6(b), with the increase of pH solution of MEFA, from 2 to 6, percentage removal and adsorption capacity also increased from 20.64% (7.37 mg/g) to 59.11% (21.92 mg/g). Thus, the optimum pH for the adsorption of MEFA by DAP-modified poly(ACN/AA) was pH 6. The pK_a value of MEFA is 4.2 (Shen et al. 2022). At pH < 4.2, MEFA molecules are protonated, while at pH > 4.2, MEFA molecules are deprotonated (Banipal, Kaur & Banipal 2017). Hence, at pH 6, highest adsorption of MEFA was obtained due to strong electrostatic attractions and H-bonding between deprotonated MEFA molecules and positively charged DAP-modified poly(ACN/AA). Low adsorption at lower pH was due to the repulsion between protonated MEFA molecules and positively charged adsorbent. As the pH continue to increase to pH 10, the adsorption of MEFA decreased to 27.77% (9.92 mg/g). This is because MEFA molecules were deprotonated and surface of adsorbent became negatively charged, resulting in electrostatic repulsive interactions.

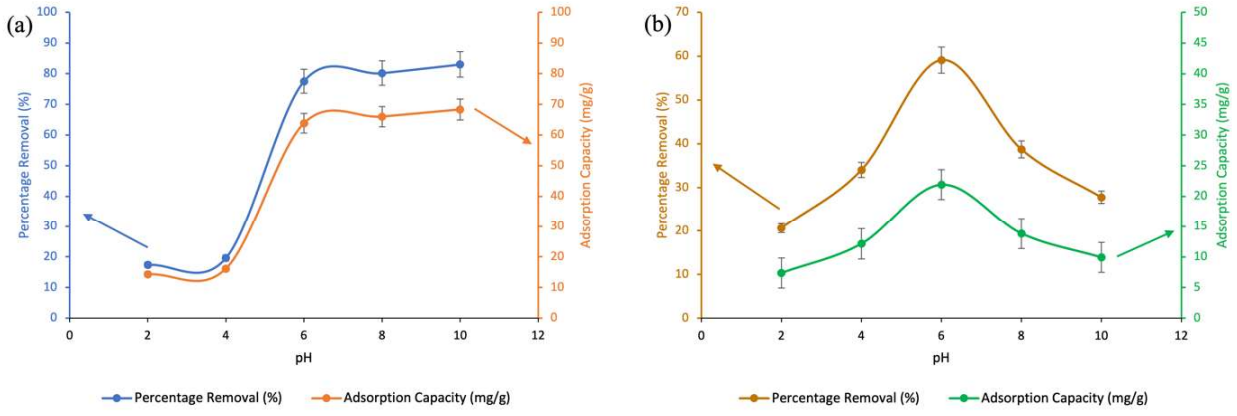

FIGURE 6. Effect of pH on percentage removal and adsorption capacity of (a) DOX and (b) MEFA

EFFECT OF ADSORBENT DOSAGE

As shown in Figure 7(a) and 7(b), the DOX and MEFA uptake by DAP-modified poly(ACN/AA), respectively, increased with the increase of adsorbent from 1 mg to 40 mg. This is associated to the increase of adsorbent surface area and excess availability of active sites for adsorption of DOX and MEFA molecules to occur as more particles of adsorbents were available in the solution (Mosoarca et al. 2020). Meanwhile, the adsorption capacity decreased as the adsorbent dosage increases. This might be due to the aggregation and agglomeration of the adsorbent particles, as the excess and suspended particles become close to each other and tend to overlap, leading to a decrease of surface area as well as active sites (Mosoarca et al. 2020). However, when 50 mg of adsorbent was used, the percentage removal slightly decreased, which might be due to the agglomeration and overlapping of adsorbent particles as the dose was high in the solution, resulting in the decrease of surface area (Mosoarca et al. 2020).

EFFECT OF CONTACT TIME

As shown in Figure 8(a) and 8(b), the percentage removal and adsorption capacity increased significantly as the contact time increased until equilibrium was achieved at 120th min. The initial rapid increase may be due to high availability of adsorbent vacant active sites for the adsorption of adsorbate molecules (Mosoarca et al. 2020). Reaching the equilibrium, the available active sites gradually filled up by the adsorbate molecules and adsorbent became saturated, leading to the slow increase of percentage removal and adsorption capacity (Mosoarca et al. 2020). Therefore, when equilibrium was achieved, no available active sites left on adsorbent surface to adsorb the remaining adsorbate molecules in the solution. For DOX, the percentage removal at 120th min was 80.21% (55.90 mg/g) and 66.08% (28.20 mg/g) for MEFA.

EFFECT OF INITIAL CONCENTRATION

Figure 9(a) and 9(b) shows the effect of DOX and MEFA concentrations on the percentage removal and adsorption capacity towards DAP-modified poly(ACN/AA), respectively. As the initial concentration of DOX and MEFA increases, the percentage removal decreases from 88.70% to 66.02% and from 69.23% to 66.95%, respectively. These results show that all active sites of DAP-modified poly(ACN/AA) were saturated with adsorbate molecules at low concentration and only few molecules were left in the solution (Adeyi et al. 2019). However, when the concentration increases, more adsorbate molecules were present in the solution, but the molecules were unable to be taken up by adsorbent since it is already saturated, resulting in more adsorbate molecules left in the solution. Contrarily, the adsorption capacity of DOX and MEFA increased from 23.14 mg/g to 185.87 mg/g and from 2.82 mg/g to 55.84 mg/g, respectively, as the initial concentration of DOX and MEFA increases. This behaviour can be explained by the increase of the driving force due to the difference in concentration gradient between DAP-modified poly(ACN/AA) phase (solid phase) and adsorbate in aqueous phase . In addition, increasing the initial concentration of adsorbate means more DOX/MEFA molecules surrounding the active sites of DAP-modified poly(ACN/AA) resulting in more collision between adsorbate and adsorbent (Adeyi et al. 2019; Mosoarca et al. 2020).

ADSORPTION ISOTHERMS

Table 4 shows the calculated isotherm parameters (q_{max}, K_L, K_F, and 1/n) and correlation coefficients, R^2 for

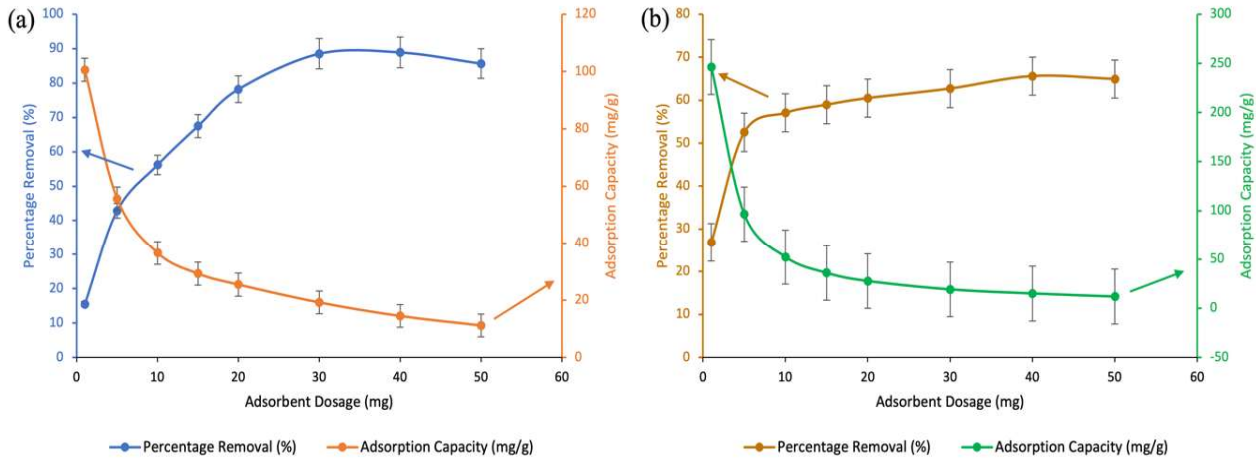

FIGURE 7. Effect of adsorbent dosage on percentage removal and adsorption capacity of (a) DOX and (b) MEFA

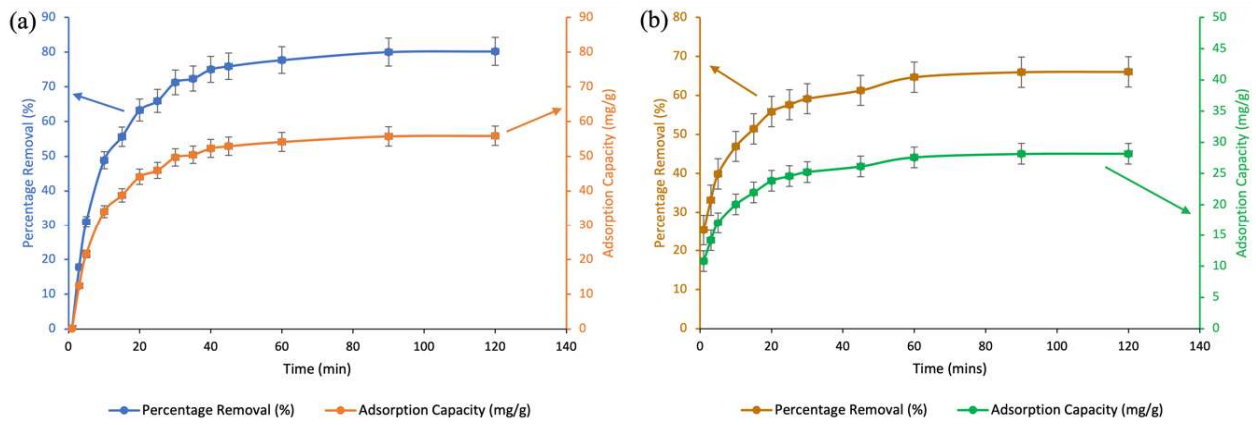

FIGURE 8. Effect of contact time on percentage removal and adsorption capacity of (a) DOX and (b) MEFA

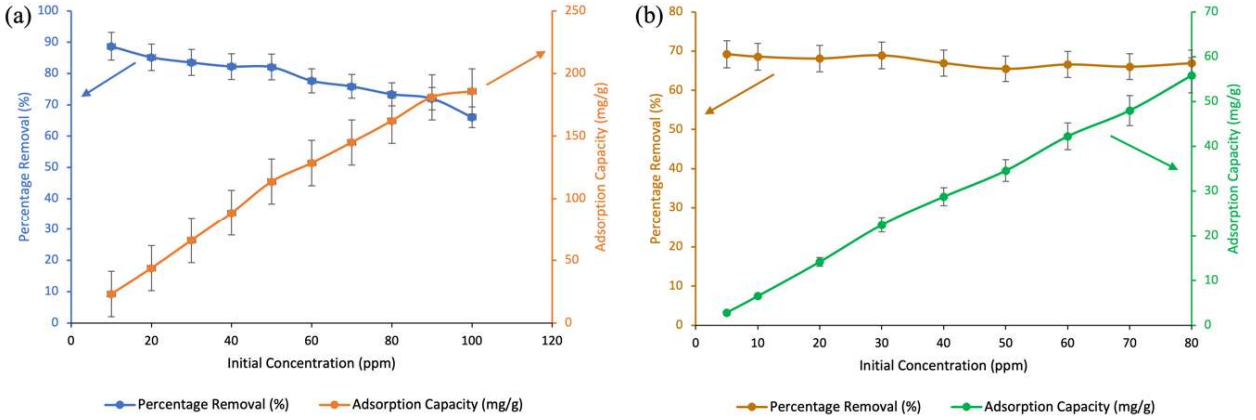

FIGURE 9. Effect of initial concentration of (a) DOX and (b) MEFA on percentage removal and adsorption capacity

TABLE 4. Isotherm parameters of DOX and MEFA adsorption by DAP-modified poly(ACN/AA)

Drugs	Isotherm Models					
	Langmuir		Freundlich		Temkin	
DOX	q_{max} (mg/g)	210.42	K_F (L/mg)	23.03	B_T (J/mol)	51.601
	K_L (mg/g)	0.1015	1/n	0.6217	K_T (L/g)	0.9088
	R^2	0.9897	R^2	0.9802	R^2	0.9648
MEFA	q_{max} (mg/g)	313.73	K_F (L/mg)	2.31	B_T (J/mol)	16.433
	K_L (mg/g)	0.0072	1/n	0.9530	K_T (L/g)	0.5663
	R^2	0.9998	R^2	0.9988	R^2	0.8705

Langmuir, Freundlich and Temkin isotherm models. Langmuir isotherm model showed the greatest R^2 value for both DOX and MEFA drugs. Therefore, the adsorption by DAP-modified poly(ACN/AA) is well fitted into the Langmuir model, suggesting that the DOX and MEFA molecules form monolayer coverage on the homogeneous surface of DAP-modified poly(ACN/AA). Moreover, the R_L value ranged from 0.4857 to 0.0805 (DOX) and 0.9714 to 0.6242 (MEFA), which indicates a favourable adsorption process (Ajenifuja, Ajao & Ajayi 2017). Freundlich isotherm model with R^2 value 0.9802 (DOX) and 0.9988 (MEFA) have $\frac{1}{n}$ value of 0.6217 for DOX and 0.9530 for MEFA. These values support that the adsorption of DOX and MEFA molecules onto DAP-modified poly(ACN/AA) was favourable because $0 < \frac{1}{n} < 1$ indicates favourable adsorption process (Adeyi et al. 2019).

The application of the Temkin model confirmed the exothermic nature of the adsorption process with heat of adsorption of 51.60 J/mol (DOX) and 16.43 J/mol (MEFA). A positive value of B_T indicates an exothermic adsorption process (Saber et al. 2021). Furthermore, the value is less than 8 kJ/mol, suggesting that the adsorption process is physical. In summary, the adsorption isotherm of DOX and MEFA molecules onto DAP-modified poly(ACN/AA) has its fitness in the following order: Langmuir model > Freundlich model > Temkin model. The maximum adsorption capacity of DOX and MEFA measured by Langmuir model were 210.42 mg/g and 313.73 mg/g, respectively. Table 5 compares the adsorption capacities of various adsorbents with DAP-modified poly(ACN/AA) towards DOX and MEFA, respectively. It is proven that DAP-modified poly(ACN/AA) records the highest adsorption capacity compared to other adsorbents.

ADSORPTION KINETICS

Table 6 shows the adsorption kinetic parameters and correlation coefficients, R^2. The adsorption of DOX and MEFA by DAP-modified poly(ACN/AA) is better fitted to PSO kinetic model based on R^2 value for both DOX and MEFA than PFO kinetic model. Furthermore, theoretical adsorption capacity, $q_{e(cal)}$ showed great difference from its corresponding experimental value at equilibrium, $q_{e(exp)}$ for PFO. Meanwhile, PSO model showed a closer value of the $q_{e(cal)}$ and $q_{e(exp)}$. This suggest that DOX and MEFA sequestration mechanism is largely dominated by chemisorption, which involves strong chemical interaction of H-bonding and ionic bonding formation between adsorbate and the surface of adsorbent (Deng et al. 2019; Pourhakkak et al. 2021).

PROPOSED MECHANISM OF DOX AND MEFA ADSORPTION BY DAP-MODIFIED POLY(ACN/AA)

Figure 10 represents the mechanism of adsorption of DOX and MEFA by DAP-modified poly(ACN/AA). DOX is a broad-spectrum antibiotic with a negatively charged ion (anion) at physiological pH. Due to the fact that the modified copolymer (adsorbent) has a pH_{PZC} of 7.88, therefore, at pH above 7.88, the adsorbent surface is negatively charged. Given that optimum adsorption occurred at pH 10 where both adsorbent and adsorbate were negatively charged, the adsorption was due to DOX molecules contain abundant hydroxyl groups that were not deprotonated (Savadi et al. 2022) which contributes to hydrogen bonding (H-O, H-N). Attractive forces between H atom covalently bonded to a very electronegative atom (N, O atom) and other electronegative atom on adsorbent surface and adsorbate

TABLE 5. Comparisons of adsorption capacity between various adsorbents and DAP-modified poly(ACN/AA) towards DOX and MEFA

Adsorbent	Adsorbate	Adsorption capacity, q_{max} (mg/g)	Reference
DAP-modified poly(ACN/AA)	DOX	210.42	This study
Zr-metal-organic frameworks	DOX	124.8	Ren et al. (2023)
Magnetic activated nanocomposite	DOX	52.08	Zahoor et al. (2022)
Iron loaded sludge biochar	DOX	128.98	Wei et al. (2019)
Fe_3O_4 magnetic nanoparticles	DOX	61.35	Ghaemi & Absalan (2015)
DAP-modified poly(ACN/AA)	MEFA	313.73	This study
Organo-Vts gemini surfavtant	MEFA	123.0	Shen et al. (2022)
[BTBAC][Lac]-MUiO-66-NH_2	MEFA	79.0	Wei et al. (2020)

TABLE 6. Kinetic parameters of DOX and MEFA adsorption by DAP-modified poly(ACN/AA)

Drugs	Kinetic models			
	Pseudo-first order		Pseudo-second order	
DOX	k_1 (min^{-1})	0.013	k_2 (g/mg•min)	0.0021
	$q_{e(exp)}$ (mg/g)	66.15	$q_{e(exp)}$ (mg/g)	66.15
	$q_{e(cal)}$ (mg/g)	32.05	$q_{e(cal)}$ (mg/g)	60.66
	R^2	0.6931	R^2	0.998
MEFA	k_1 (g)	0.031	k_2 (g/mg•min)	0.0089
	$q_{e(exp)}$ (mg/g)	28.71	$q_{e(exp)}$ (mg/g)	28.71
	$q_{e(cal)}$ (mg/g)	11.40	$q_{e(cal)}$ (mg/g)	29.10
	R^2	0.9226	R^2	0.9993

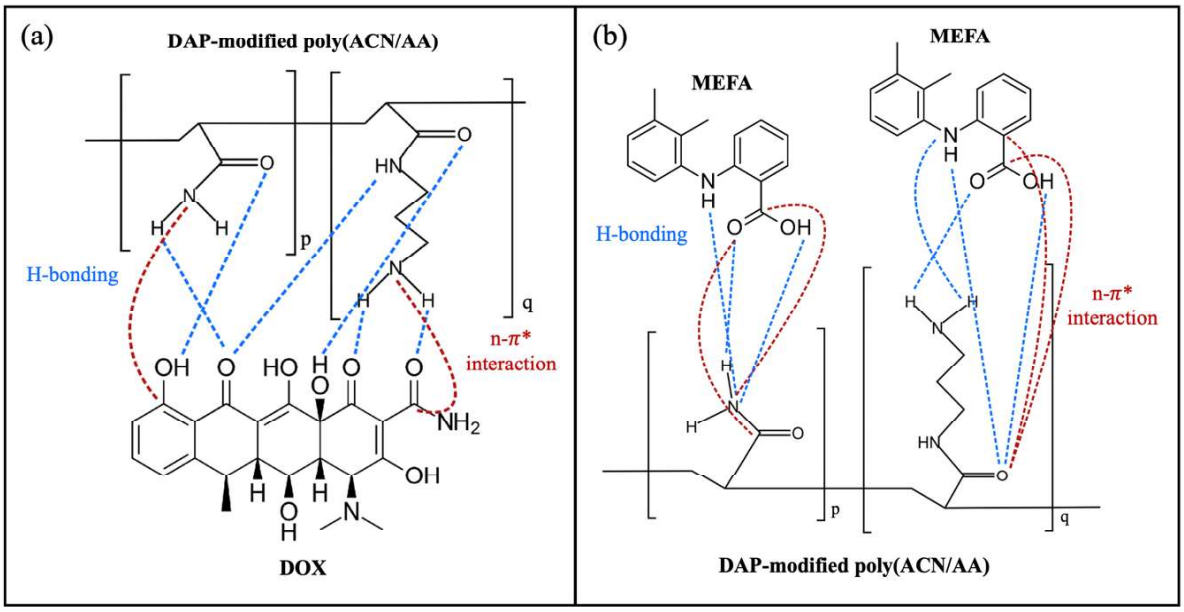

FIGURE 10. Proposed interaction mechanisms of (a) DOX and (b) MEFA towards the active sites of DAP-modified poly(ACN/AA)

molecules (Qiu et al. 2022). Moreover, as the adsorbent and adsorbates molecules contain -NH_2 (amine group), -OH (hydroxyl group), and C═O (carbonyl group), the n-π^* interaction could be formed where N or O atom (nucleophile) donate their lone pair to C atom of carbonyl group between adsorbent surface and adsorbate molecules. The n-π^* interaction is defined as when a nucleophile donates lone-pair (n) electron density into the empty π^* orbital of a nearby carbonyl group. Mixing of these orbitals releases energy, resulting in an attractive interaction (Newberry & Raines 2017). The proposed mechanism is illustrated in Figure 10(a).

Meanwhile, MEFA is a weakly acidic compound with a pK_a value of around 4.2 (Subri et al. 2018). This means that it is mostly present in its acidic form (HA) at physiological pH. At pH below 7.88, the adsorbent surface is positively charged, which would attract the negatively charged mefenamic acid anion (A^-). Given that the optimum adsorption of MEFA was at pH 6, this suggests that the adsorbent may be most effective in adsorbing MEFA as the positive charge on the adsorbent surface would interact with the negative charge on the MEFA anion due to deprotonation (Banipal, Kaur & Banipal 2017), facilitating electrostatic attraction and adsorption. As illustrated in

Figure 10(b) the carbonyl and amine functional groups on the adsorbent may interact with the carboxylic acid group of MEFA through hydrogen bonding (Qiu et al. 2022). The n-π^* interaction would also enhance the adsorption of MEFA onto the adsorbent.

CONCLUSIONS

The research presented successful synthesis of poly(ACN/AA) copolymer and its modification with DAP. The results of polymerization yields, amine density, FT-IR, SEM and BET analyses indicate that the modification of poly(ACN/AA) with DAP increased the amine content and altered the chemical structure of the polymer. The as-synthesized modified polymer was used as an adsorbent for the sequestration of DOX and MEFA antibiotics. The adsorption studies resulted in high percentage removal of doxycycline and mefenamic acid. The optimum amount of adsorbent used to adsorb DOX and MEFA was 40 mg with 120 min contact time at pH 10 and 6, respectively. This condition results in 83.02% removal of DOX and 59.11% removal of MEFA from aqueous solution. The adsorption isotherm behaviour of DOX and MEFA were best described by Langmuir isotherm model, indicating a monolayer adsorption process. The maximum Langmuir sequestration capacity was 210.40 mg/g and 313.74 mg/g for DOX and MEFA uptake, respectively. The adsorption kinetic of DOX and MEFA followed pseudo-second order model, indicating a chemisorption process. According to the outcome of this study, DAP-modified poly(ACN/AA) could be a promising and potential functional adsorbent in the separation of acidic pharmaceutical compounds from liquid phase environment.

ACKNOWLEDGEMENTS

We would like to acknowledge the Chemistry Department, Faculty of Science, Universiti Putra Malaysia (UPM), for providing resources and research facilities. The research is funded by Ministry of Higher Education (MOHE) Malaysia with grant code FRGS/1/206/TK05/UPM/02/1 (MOHE reference) and UPM reference of UPM/700-2/1/FRGS/03-01-16-1844FR.

REFERENCES

Abu Rumman, G., Al-Musawi, T.J., Sillanpaa, M. & Balarak, D. 2021. Adsorption performance of an amine-functionalized MCM–41 mesoporous silica nanoparticle system for ciprofloxacin removal. *Environmental Nanotechnology, Monitoring and Management* 16: 100536. https://doi.org/10.1016/j.enmm.2021.100536

Adeyi, A.A., Jamil, S.N.A.M., Abdullah, L.C. & Choong, T.S.Y. 2019. Adsorption of malachite green dye from liquid phase using hydrophilic thiourea-modified poly(acrylonitrile-*co*-acrylic acid): Kinetic and isotherm studies. *Journal of Chemistry* 2019: 4321475. https://doi.org/10.1155/2019/4321475

Ahmed, M.B., Zhou, J.L., Ngo, H.H., Guo, W., Johir, M.A.H. & Sornalingam, K. 2017. Single and competitive sorption properties and mechanism of functionalized biochar for removing sulfonamide antibiotics from water. *Chemical Engineering Journal* 311: 348-358. https://doi.org/10.1016/j.cej.2016.11.106

Ajenifuja, E., Ajao, J.A. & Ajayi, E.O.B. 2017. Equilibrium adsorption isotherm studies of Cu (II) and Co (II) in high concentration aqueous solutions on Ag-TiO_2-modified kaolinite ceramic adsorbents. *Applied Water Science* 7(5): 2279-2286. https://doi.org/10.1007/s13201-016-0403-6

Al-Ameer, L., Hashim, K.K. & Taha, D.N. 2022. Determination of mefenamic acid in aqueous solutions using merging zone - continuous flow injection. *Water Practice and Technology* 17(9): 1881-1892. https://doi.org/10.2166/wpt.2022.096

Al-Odaini, N.A., Zakaria, M.P., Yaziz, M.I., Surif, S. & Abdulghani, M. 2013. The occurrence of human pharmaceuticals in wastewater effluents and surface water of Langat River and its tributaries, Malaysia. *International Journal of Environmental Analytical Chemistry* 93(3): 245-264. https://doi.org/10.1080/03067319.2011.592949

Banipal, T.S., Kaur, H. & Banipal, P.K. 2017. Studies on the binding ability of diclofenac sodium to cationic surfactants micelles in aqueous ethanol solutions: Calorimetric, spectroscopic, and light scattering approach. *Journal of Thermal Analysis and Calorimetry* 128(1): 501-511. https://doi.org/10.1007/s10973-016-5889-5

Deng, F., Luo, X-B., Ding, L. & Luo, S-L. 2019. Application of nanomaterials and nanotechnology in the reutilization of metal ion from wastewater. In *Nanomaterials for the Removal of Pollutants and Resource Reutilization*, edited by Luo, X. & Deng, F. Elsevier. pp. 149-178. https://doi.org/10.1016/B978-0-12-814837-2.00005-6

Dolatabadi, M., Ahmadzadeh, S. & Ghaneian, M.T. 2020. Mineralization of mefenamic acid from hospital wastewater using electro-Fenton degradation: Optimization and identification of removal mechanism issues. *Environmental Progress and Sustainable Energy* 39(3): e13380. https://doi.org/10.1002/ep.13380

Eniola, J.O., Kumar, R., Barakat, M.A. & Rashid, J. 2022. A review on conventional and advanced hybrid technologies for pharmaceutical wastewater treatment. *Journal of Cleaner Production* 356: 131826. https://doi.org/10.1016/j.jclepro.2022.131826

Gao, F. 2019. An overview of surface-functionalized magnetic nanoparticles: Preparation and application for wastewater treatment. *ChemistrySelect* 4(22): 6805-6811. https://doi.org/10.1002/slct.201900701

Ghaemi, M. & Absalan, G. 2015. Fast removal and determination of doxycycline in water samples and honey by Fe_3O_4 magnetic nanoparticles. *Journal of the Iranian Chemical Society* 12: 1-7. https://doi.org/10.1007/s13738-014-0450-6

Habila, M.A., Moshab, M.S., El-Toni, A.M., ALOthman, Z.A. & Badjah Hadj Ahmed, A.Y. 2023. Thermal fabrication of magnetic Fe_3O_4 (nanoparticle)@carbon sheets from waste resources for the adsorption of dyes: Kinetic, equilibrium, and UV–visible spectroscopy investigations. *Nanomaterials* 13(7): 1266. https://doi.org/10.3390/nano13071266

Hanafiah, Z.M., Bithi, A.S., Mohtar, W.H.M.W., Zin, W.Z.W., Tahrim, N.A., Manan, T.S.A., Rohani, R. & Indarto, A. 2024. Pharmaceutical footprint in domestic wastewater: Case study in Malaysia. *Water, Air, & Soil Pollution* 235: 51. https://doi.org/10.1007/s11270-023-06844-1

Hassan, M.M. & Hawkyard, C.J. 2007. Decolorisation of effluent with ozone and re-use of spent dyebath. In *Environmental Aspects of Textile Dyeing*, edited by Christie, R. Elsevier. pp. 149-190. https://doi.org/10.1533/9781845693091.149

Hua, Y., Yao, Q., Lin, J., Li, X. & Yang, Y. 2022. Comprehensive survey and health risk assessment of antibiotic residues in freshwater fish in southeast China. *Journal of Food Composition and Analysis* 114: 104821. https://doi.org/10.1016/j.jfca.2022.104821

Husien, S., El-Taweel, R.M., Salim, A.I., Fahim, I.S., Said, L.A. & Radwan, A.G. 2022. Review of activated carbon adsorbent material for textile dyes removal: Preparation, and modelling. *Current Research in Green and Sustainable Chemistry* 5: 100325. https://doi.org/10.1016/j.crgsc.2022.100325

Ismar, E. & Sarac, A.S. 2016. Synthesis and characterization of poly (acrylonitrile-co-acrylic acid) as precursor of carbon nanofibers. *Polymers for Advanced Technologies* 27(10): 1383-1388. https://doi.org/10.1002/pat.3807

Jamil, S., Daik, R. & Ahmad, I. 2014. Synthesis and thermal properties of acrylonitrile/butyl acrylate/fumaronitrile and acrylonitrile/ethyl hexyl acrylate/fumaronitrile terpolymers as a potential precursor for carbon fiber. *Materials* 7(9): 6207-6223. https://doi.org/10.3390/ma7096207

Lai, E.C., Shin, J., Kubota, K., Man, K.K.C., Park, B.J., Pratt, N., Roughead, E.E., Wong, I.C.K., Kao Yang, Y. & Setoguchi, S. 2018. Comparative safety of NSAIDs for gastrointestinal events in Asia-Pacific populations: A multi-database, international cohort study. *Pharmacoepidemiology and Drug Safety* 27(11): 1223-1230. https://doi.org/10.1002/pds.4663

Malaysian Health Technology Assessment Section. 2022. Putrajaya: Ministry of Health Malaysia. https://hq.moh.gov.my/medicaldev/cawangan-penilaian-teknologi-kesihatan/

McMurry, J.E. 2023. *Organic Chemistry: A Tenth Edition*. OpenStax.

Mohamad, Z.A., Md Jamil, S.N.A., Subri, N.N.S., Ismail, F.S. & Daik, R. 2023. Adsorption of diclofenac from aqueous solution by amine-functionalized poly (acrylonitrile-co-acrylic acid) microparticles adsorbent. *Sains Malaysiana* 52(11): 3189-3209. https://doi.org/10.17576/jsm-2023-5211-13

Mohd Hanafiah, Z., Wan Mohtar, W.H.M., Abd Manan, T.S., Bachi, N.A., Abu Tahrim, N., Abd Hamid, H.H., Ghanim, A., Ahmad, A., Wan Rasdi, N. & Abdul Aziz, H. 2023. Determination and risk assessment of pharmaceutical residues in the urban water cycle in Selangor Darul Ehsan, Malaysia. *PeerJ* 11: e14719. https://doi.org/10.7717/peerj.14719

Mosoarca, G., Vancea, C., Popa, S., Gheju, M. & Boran, S. 2020. *Syringa vulgaris* leaves powder a novel low-cost adsorbent for methylene blue removal: Isotherms, kinetics, thermodynamic and optimization by Taguchi method. *Scientific Reports* 10: 17676. https://doi.org/10.1038/s41598-020-74819-x

Mudhoo, A., Bhatnagar, A., Rantalankila, M., Srivastava, V. & Sillanpää, M. 2019. Endosulfan removal through bioremediation, photocatalytic degradation, adsorption and membrane separation processes: A review. *Chemical Engineering Journal* 360: 912-928. https://doi.org/10.1016/j.cej.2018.12.055

Nandiyanto, A.B.D., Ragadhita, R. & Fiandini, M. 2023. Interpretation of Fourier transform infrared spectra (FTIR): A practical approach in the polymer/plastic thermal decomposition. *Indonesian Journal of Science and Technology* 8(1): 113-126. https://doi.org/10.17509/ijost.v8i1.53297

Newberry, R.W. & Raines, R.T. 2017. The n→π∗ interaction. *Accounts of Chemical Research* 50(8): 1838-1846. https://doi.org/10.1021/acs.accounts.7b00121

Olusegun, S.J. & Mohallem, N.D.S. 2019. Insight into the adsorption of doxycycline hydrochloride on different thermally treated hierarchical $CoFe_2O_d$/bio-silica nanocomposite. *Journal of Environmental Chemical Engineering* 7(6): 103442. https://doi.org/10.1016/j.jece.2019.103442

Panic, V., Seslija, S., Nesic, A. & Velickovic, S. 2013. Adsorption of azo dyes on polymer materials. *Hemijska Industrija* 67(6): 881-900. https://doi.org/10.2298/HEMIND121203020P

Perumal, M.K.K., Gandhi, D., Renuka, R.R., Lakshminarayanan, A., Thiyagarajulu, N. & Kamaraj, C. 2024. Advanced nano-based adsorbents for purification of pharmaceutical residue polluted water: A critical review. *Process Safety and Environmental Protection* 186: 552-565. https://doi.org/10.1016/j.psep.2024.04.011

Pourhakkak, P., Taghizadeh, A., Taghizadeh, M., Ghaedi, M. & Haghdoust, S. 2021. Fundamentals of adsorption technology. *Interface Science and Technology* 33: 1-70. https://doi.org/10.1016/B978-0-12-818805-7.00001-1

Qiu, B., Shao, Q., Shi, J., Yang, C. & Chu, H. 2022. Application of biochar for the adsorption of organic pollutants from wastewater: Modification strategies, mechanisms and challenges. *Separation and Purification Technology* 300: 121925. https://doi.org/10.1016/j.seppur.2022.121925

Rahimi, K., Riahi, S., Abbasi, M. & Fakhroueian, Z. 2019. Modification of multi-walled carbon nanotubes by 1,3-diaminopropane to increase CO_2 adsorption capacity. *Journal of Environmental Management* 242: 81-89. https://doi.org/10.1016/j.jenvman.2019.04.036

Rapeia, N.S.M., Jamil, S.N.A.M., Abdullah, L.C., Mobarekeh, M.N., Yaw, T.C.S., Huey, S.J. & Zahri, N.A.M. 2014. Preparation and characterization of hydrazine-modified poly(acrylonitrile-co-acrylic acid). *Journal of Engineering Science and Technology Special Issue on SOMCHE 2014 & RSCE 2014 Conference*. pp. 61-70.

Ren, Q., Ma, Y., Wei, F., Qin, L., Chen, H., Liang, Z. & Wang, S. 2023. Preparation of Zr-MOFs for the adsorption of doxycycline hydrochloride from wastewater. *Green Processing and Synthesis* 12(1): 20228127. https://doi.org/10.1515/gps-2022-8127

Saber, S.E., Abdullah, L.C., Md. Jamil, S.N.A., Choong, T.S.Y. & Ting, T.M. 2021. Trimethylamine functionalized radiation-induced grafted polyamide 6 fibers for p-nitrophenol adsorption. *Scientific Reports* 11: 19573. https://doi.org/10.1038/s41598-021-97397-y

Samal, K., Mahapatra, S. & Hibzur Ali, M. 2022. Pharmaceutical wastewater as emerging contaminants (EC): Treatment technologies, impact on environment and human health. *Energy Nexus* 6: 100076. https://doi.org/10.1016/j.nexus.2022.100076

Santos, D., Costa, F., Franceschi, E., Santos, A., Dariva, C. & Mattedi, S. 2014. Synthesis and physico-chemical properties of two protic ionic liquids based on stearate anion. *Fluid Phase Equilibria* 376: 132-140. https://doi.org/10.1016/j.fluid.2014.05.043

Savadi, P., Lotfipour, F., McMillan, N.A.J., Hashemzadeh, N. & Hallaj-Nezhadi, S. 2022. Passive and pH-gradient loading of doxycycline into nanoliposomes using modified freeze-drying of a monophase solution method for enhanced antibacterial activity. *Chemical Papers* 76(5): 3097-3108. https://doi.org/10.1007/s11696-021-02036-5

Shen, T., Han, T., Zhao, Q., Ding, F., Mao, S. & Gao, M. 2022. Efficient removal of mefenamic acid and ibuprofen on organo-Vts with a quinoline-containing gemini surfactant: Adsorption studies and model calculations. *Chemosphere* 295: 133846 https://doi.org/10.1016/j.chemosphere.2022.133846

Slavov, D., Tomaszewska, E., Grobelny, J., Drenchev, N., Karashanova, D., Peshev, Z. & Bliznakova, I. 2024. FTIR spectroscopy revealed nonplanar conformers, chain order, and packaging density in diOctadecylamine- and octadecylamine-passivated gold nanoparticles. *Journal of Molecular Structure* 1314: 138827. https://doi.org/10.1016/j.molstruc.2024.138827

Sruthi, P.R. & Anas, S. 2020. An overview of synthetic modification of nitrile group in polymers and applications. *Journal of Polymer Science* 58(8): 1039-1061. https://doi.org/10.1002/pol.20190190

Subri, N.N.S., Cormack, P.A.G., Siti Nurul, S.N.A., Abdullah, L.C. & Daik, R. 2018. Synthesis of poly(acrylonitrile-co-divinylbenzene-co-vinylbenzyl chloride)-derived hypercrosslinked polymer microspheres and a preliminary evaluation of their potential for the solid-phase capture of pharmaceuticals. *Journal of Applied Polymer Science* 135(2): 45677. https://doi.org/10.1002/app.45677

Thiang, E.L., Lee, C.W., Takada, H., Seki, K., Takei, A., Suzuki, S., Wang, A. & Bong, C.W. 2021. Antibiotic residues from aquaculture farms and their ecological risks in Southeast Asia: A case study from Malaysia. *Ecosystem Health and Sustainability* 7(1): 1926337. https://doi.org/10.1080/20964129.2021.1926337

Wang, J. & Guo, X. 2020. Adsorption kinetic models: Physical meanings, applications, and solving methods. *Journal of Hazardous Materials* 390: 122156. https://doi.org/10.1016/j.jhazmat.2020.122156

Wei, J., Liu, Y., Li, J., Zhu, Y., Yu, H. & Peng, Y. 2019. Adsorption and co-adsorption of tetracycline and doxycycline by one-step synthesized iron loaded sludge biochar. *Chemosphere* 236: 124254. https://doi.org/10.1016/j.chemosphere.2019.06.224

Wei, X., Wang, Y., Chen, J., Xu, F., Liu, Z., He, X., Li, H. & Zhou, Y. 2020. Adsorption of pharmaceuticals and personal care products by deep eutectic solvents-regulated magnetic metal-organic framework adsorbents: Performance and mechanism. *Chemical Engineering Journal* 392: 124808. https://doi.org/10.1016/j.cej.2020.124808

World Health Organization (WHO). 2023. *Antimicrobial Resistance*. Geneva: World Health Organization.

Yadav, S., Shah, A. & Malhotra, P. 2024. Orange peel-derived Cu_2O/RGO nanocomposite: Mesoporous binary system for degradation of doxycycline in water. *Environment, Development and Sustainability* 26(2): 4505-4532. https://doi.org/10.1007/s10668-022-02895-2

Yadav, K., Latelwar, S.R., Datta, D. & Jana, B. 2023. Efficient removal of MB dye using litchi leaves powder adsorbent: Isotherm and kinetic studies. *Journal of the Indian Chemical Society* 100(4): 100974. https://doi.org/10.1016/j.jics.2023.100974

Zahoor, M., Wahab, M., Salman, S.M., Sohail, A., Ali, E.A. & Ullah, R. 2022. Removal of doxycycline from water using *Dalbergia sissoo* waste biomass based activated carbon and magnetic oxide/activated bioinorganic nanocomposite in batch adsorption and adsorption/membrane hybrid processes. *Bioinorganic Chemistry and Applications* 2022: 2694487. https://doi.org/10.1155/2022/2694487

Zahri, N.A.M., Jamil, S.N.A.M., Abdullah, L.C., Yaw, T.C.S., Mobarekeh, M.N., Huey, S.J. & Rapeia, N.S.M. 2015. Improved method for preparation of amidoxime modified poly(acrylonitrile-co-acrylic acid): Characterizations and adsorption case study. *Polymers* 7(7): 1205-1220. https://doi.org/10.3390/polym7071205

*Corresponding author; email: ctnurulain@upm.edu.my